Journal of Integrative Neuroscience

J. Integr. Neurosci. **2026**; 25(5): 47320
https://doi.org/10.31083/JIN47320

Original Research

Metabolic Brain Network Reorganization in Temporal Lobe Epilepsy With Aware or Impaired Awareness Seizures

Jingke Xiao[1,†], Fan Yang[1,†], Hanlin Zhang[1], Jiangyan Liu[1,*]

[1]Department of Nuclear Medicine, The Second Hospital & Clinical Medical School, Lanzhou University, 730030 Lanzhou, Gansu, China
*Correspondence: ery_liujy@lzu.edu.cn (Jiangyan Liu)
[†]These authors contributed equally.

Academic Editor: Bettina Platt
Submitted: 13 October 2025 Revised: 9 January 2026 Accepted: 9 February 2026 Published: 9 May 2026

Abstract

Background: Temporal lobe epilepsy (TLE) is increasingly recognized as a dysfunction of the brain network. However, the topological alterations of the metabolic brain network underlying impaired awareness seizures (IAS) remain unclear. In this study, we aimed to characterize metabolic network reorganization in patients with TLE and IAS (TLE-IAS) and to preliminarily investigate the specificity of these alterations by comparing the results with those of patients with TLE and aware seizures (AS). **Methods**: This retrospective study included a total of 193 TLE-IAS patients, 30 patients with TLE-AS, and 193 controls. Metabolic brain networks were constructed for all groups, and nonparametric permutation testing was applied to compare group differences in graph-theoretical metrics and hub node distribution. **Results**: Compared with controls, both TLE patient groups exhibited globally weakened metabolic connectivity. Graph-theoretical analysis revealed that both groups demonstrated significant increases in characteristic path length and significant decreases in clustering coefficient (Cp). Furthermore, the TLE-AS group showed a significant decrease in local efficiency compared with controls. No statistically significant differences were found between the two patient groups across the four graph-theoretical parameters. Hub analysis revealed a convergent reorganization in both groups involving loss of default mode network hubs and a limbic/paralimbic shift, with the TLE-IAS group showing more limbic hubs, while the TLE-AS group exhibited more primary auditory hubs. **Conclusions**: This study revealed alterations in graph-theoretical parameters and hub distribution in patients with TLE-IAS and TLE-AS. These findings provide preliminary metabolic imaging evidence for the neural substrates underlying impaired awareness in TLE.

Keywords: epilepsy; temporal lobe; positron emission tomography; neural pathways

1. Introduction

Epilepsy is a chronic brain disorder marked by recurrent, unprovoked seizures [1]. Based on awareness per the 2017 International League Against Epilepsy (ILAE) classification, focal seizures are categorized as focal impaired awareness seizures (IAS) and focal aware seizures (AS) [2]. IAS are characterized by diminished awareness, manifested as reduced overall arousal and responsiveness. AS refer to the patient's ability to remain conscious of both self and environment during an epileptic seizure, even if motor responsiveness is impaired. Although IAS increases the risk of accidental injuries such as traffic accidents, drowning, and falls in patients, its mechanism remains unclear at present [3]. Temporal lobe epilepsy (TLE), the most common form of focal epilepsy, is frequently associated with IAS.

To investigate functional connectivity, methods such as correlation, coherence, or component analysis [4] are typically applied to functional neuroimaging data [e.g., electroencephalography (EEG), magnetoencephalography (MEG), functional magnetic resonance imaging (fMRI), or positron emission tomography (PET)]. It is a conceptual class comprising multiple distinct members [5]. Metabolic connectivity, defined as a set of statistical interrelationships in metabolic values (primarily measured by PET) between different brain regions, is considered a specific form of functional connectivity [6]. PET is a noninvasive modality that quantitatively measures cerebral glucose levels using radiotracers such as ^{18}F-fluorodeoxyglucose (^{18}F-FDG) [7], where the signals are generated by the coupling between synaptic transmission and local glucose consumption [8]. Therefore, the correlation of glucose uptake between different brain regions can reflect the strength of their functional connectivity. In magnetic resonance imaging (MRI)-negative epilepsy patients, PET can sensitively identify epileptogenic zones and abnormal metabolic networks, serving as an important noninvasive adjunct for localizing epileptogenic foci and guiding clinical management [9].

Epilepsy is caused by brain network dysfunction. Brain network analysis methods, which are widely applied to study neurodevelopmental and neurodegenerative disorders, are important tools in epilepsy research [10,11]. Numerous studies have demonstrated that during ictal and interictal periods, the propagation of abnormal discharges significantly alters whole-brain functional connectivity, resulting in network dysfunction [12–14]. Graph theory-based network analysis can be used to effectively quantify such network abnormalities [15,16]. Regarding the mechanisms underlying impaired awareness in epilepsy, Bartolomei and

Naccache [17] postulated the "global workspace theory" and noted that fronto-parietal associative cortices are key factors in severe awareness alterations during seizures. Additionally, Yu and Blumenfeld [18] proposed the network inhibition hypothesis to describe impaired awareness in TLE, suggesting that TLE disrupts the upper brain stem-diencephalic activating systems, leading to decreased activity or inhibition of the fronto-parietal association cortex. Previous studies using diverse technical approaches have implicated potential neural substrates in TLE-IAS. On the one hand, diffusion tensor imaging studies indicate that the thalamus and upper brainstem may play critical roles in epileptic patients with impaired awareness [19]. On the other hand, Campora *et al*. [20] used stereo-EEG to demonstrate that TLE-IAS involves hippocampal activity at all points during seizures. However, how static metabolic networks specifically manifest the differences between TLE-IAS and TLE-AS has not yet been systematically investigated.

Current PET research on TLE-IAS primarily focuses on alterations in regional metabolic patterns [21], overlooking the critical comparison with TLE-AS patients. Notably, the maintenance of consciousness relies on the integrated functioning of whole-brain networks [22]. Therefore, localized metabolic analyses, coupled with the lack of comparative data with TLE-AS patients, are inadequate to elucidate the specific network-level mechanisms underlying impaired awareness. To this end, this study aims to construct metabolic brain networks for patients with TLE-IAS or TLE-AS and controls. The subsequent quantitative analyses of graph-theoretical properties and hub distributions are designed to characterize the specific network reorganization patterns in TLE-IAS, thereby elucidating the neural basis of impaired awareness.

2. Materials and Methods

2.1 General Clinical Data

This retrospective study included patients with TLE-IAS or TLE-AS who underwent cerebral ^{18}F-FDG PET/computed tomography (CT) examinations at the Department of Nuclear Medicine, Lanzhou University Second Hospital, between January 2018 and January 2025.

The inclusion criteria were as follows: patients aged between 6 and 65 years; complete clinical data with a documented history of impaired awareness seizures (i.e., reduced responsiveness to verbal commands during seizures or inability to recall the ictal episode) or aware seizures; a confirmed clinical diagnosis of TLE; and no seizures occurring within 24 hours before or during the PET scan. The exclusion criteria included: indeterminate seizure type; MRI evidence of major structural abnormalities, such as encephalitis, cerebral infarction, intracerebral hemorrhage, cerebrovascular malformation, or intracranial tumor (except hippocampal sclerosis); prior intracranial surgery; severe metabolic disorders; or neuropsychiatric illness.

Based on these criteria, 30 patients with TLE-AS and 193 patients with TLE-IAS were enrolled. The control group consisted of 193 individuals, who were matched to the TLE-IAS group for age and sex. All controls underwent PET/CT during the same period and had no history of central nervous system diseases (e.g., healthy subjects or patients with non-neurological disorders). We systematically collected demographic data (age, sex), clinical characteristics (onset age and duration of seizures), and brain MRI findings for all enrolled patients.

2.2 ^{18}F-FDG PET Image Acquisition and Preprocessing

All PET/CT scans were performed using a Discovery 690 scanner (GE Healthcare, Waukesha, WI, USA). For patients with epilepsy, the scans were performed during an interictal period, which was confirmed by continuous clinical observation for at least 24 hours before and throughout the PET scanning procedure. All subjects fasted for at least 6 hours before the examination, ensuring fasting blood glucose levels between 3.9 and 6.3 mmol/L. Subsequently, 2.96–5.55 MBq/kg of ^{18}F-FDG was administered intravenously, followed by a 40–60 minute rest period in a quiet, dimly lit room for all participants. PET/CT imaging was then performed in the supine position. Brain PET acquisition lasted 5 minutes per bed position. A low-dose CT scan was first acquired using the following parameters: slice thickness, 3.75 mm; tube current, 50–220 mA; tube voltage, 120 kV; and matrix size, 512 $\times$ 512. PET data were then acquired in 3D+time-of-flight (TOF) mode with a matrix size of 256 $\times$ 256 and reconstructed using the VUE Point FX algorithm (18 subsets, 4 iterations).

Image preprocessing was conducted using Statistical Parametric Mapping (SPM12, Wellcome Trust Centre for Neuroimaging, London, UK) running on MATLAB R2022a (MathWorks, Natick, MA, USA). After converting the DICOM-format PET images into NIfTI format, the origin coordinates were manually adjusted. All individual PET images were then spatially normalized to the Montreal Neurological Institute (MNI) PET template provided in SPM12 and resampled to a voxel size of 2 $\times$ 2 $\times$ 2 mm^3.

2.3 Construction and Analysis of PET Metabolic Brain Networks

The PET metabolic brain networks were constructed and analyzed as follows. Preprocessed PET images from the TLE-IAS, TLE-AS, and control groups were parcellated into regions of interest using the Automated Anatomical Labeling 90 atlas. This divided the whole brain into 90 anatomical regions that served as network nodes. The standardized uptake value (SUV) of each region was calculated. The cerebellum—which exhibits relatively stable glucose metabolism—was used as a reference region to obtain the standardized uptake value ratio (SUVR) for each region [23,24].

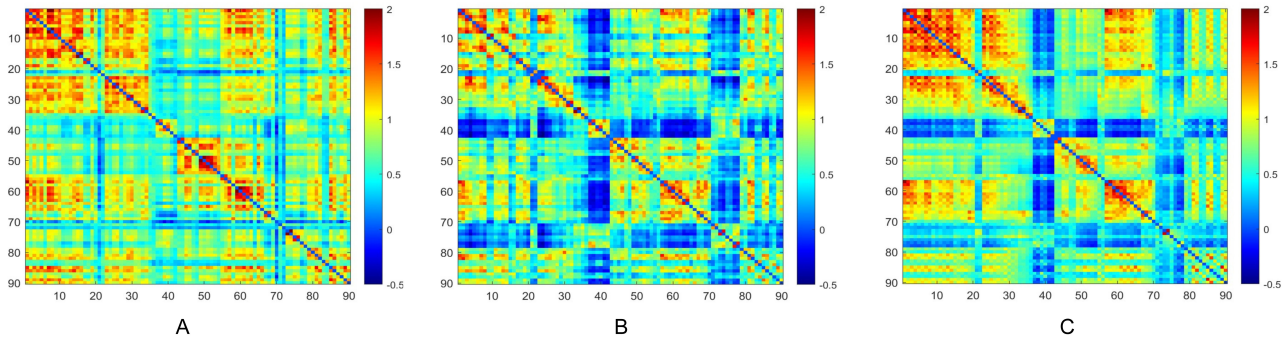

Fig. 1. Metabolic connectivity matrices of brain networks in the three groups. (A) Control group, (B) TLE-AS, and (C) TLE-IAS groups. TLE-AS, temporal lobe epilepsy-aware seizures; TLE-IAS, temporal lobe epilepsy-impaired awareness seizures.

At the group level, Pearson correlation coefficients between all pairs of the 90 brain regions (retaining only positive correlations) were computed separately for the TLE-IAS, TLE-AS, and control groups, generating three 90 × 90 correlation matrices. To optimize the network topology, each correlation matrix was binarized across a sparsity range of 0.25–0.75 (incremented by 0.01) [24,25].

Subsequently, global and nodal network metrics were computed using GRETNA 2.0 (https://www.nitrc.org/projects/gretna/), including characteristic path length (Lp), clustering coefficient (Cp), global efficiency (Eg), local efficiency (Eloc), and betweenness centrality (Bc) [26,27]. Hub nodes were identified as those with a normalized betweenness centrality (Bc/mean Bc) greater than 2 and statistically significant according to permutation testing [28,29]. Visualization of hub node distributions was performed using BrainNet Viewer (https://www.nitrc.org/projects/bnv/) [30].

2.4 Statistical Analysis

Statistical analyses were performed using SPSS 25.0 (IBM Corp., Armonk, NY, USA) and MATLAB R2022a. Continuous variables following a normal distribution were presented as mean ± standard deviation (SD). For intergroup comparisons, the *t*-test was used. Categorical data were summarized as proportions and compared using the chi-squared test. Non-normally distributed continuous data are presented as median (interquartile range) [M (IQR)], and comparisons between two groups were performed using the Mann-Whitney U test. Group differences in PET-based metabolic network metrics were assessed using nonparametric permutation tests (1000 iterations) supplemented by bootstrap resampling (1000 iterations) for robustness validation. The false discovery rate (FDR) correction was applied to control for multiple comparisons in hub node identification. A two-sided $p < 0.05$ was considered statistically significant.

3. Results

3.1 Participant Characteristics

No significant differences in demographic or clinical characteristics (age, sex, onset age of seizure, duration of seizure, and MRI findings) were found between the TLE-AS group and the other two groups (all $p > 0.05$) (Table 1).

3.2 Construction of PET Metabolic Brain Networks

Metabolic connectivity matrices for the TLE-IAS and control groups were constructed by calculating Pearson correlation coefficients of glucose metabolism across all brain regions (Fig. 1). The interregional metabolic connections of both groups were visualized, with the color bar representing correlation strength. The TLE-IAS and TLE-AS groups tended to exhibit weaker metabolic connectivity compared to the control group, suggesting reduced interregional coordination of glucose metabolism. Additionally, we generated metabolic connectivity difference matrices comparing each patient group (TLE-IAS and TLE-AS) with the control group to visualize alterations (**Supplementary Fig. 1**).

3.3 Graph Theory Analysis of Brain Networks

Within the sparsity range of 0.25–0.75, graph-theoretical analysis of the metabolic networks revealed alterations in global and local properties across all groups. Compared with the control group, the TLE-IAS group exhibited significantly increased Lp and decreased Cp, with no significant differences in Eg and Eloc (Fig. 2). After FDR correction for each sparsity level, significant between-group differences were observed for Lp at certain sparsity levels (0.47–0.52, 0.58–0.75) (p_{FDR} ranging from 0.044 to 0.048, mean ΔLp: –0.1436), whereas Cp showed significant intergroup differences at specific sparsity levels (0.34, 0.37, 0.38, 0.42–0.75) (p_{FDR} ranging from 0.003 to 0.036, mean ΔCp: 0.0880). No significant intergroup differences were observed for Eg and Eloc across all sparsity levels (all $p_{FDR} > 0.05$).

Compared with the control group, the TLE-AS group exhibited significantly increased Lp and significantly de-

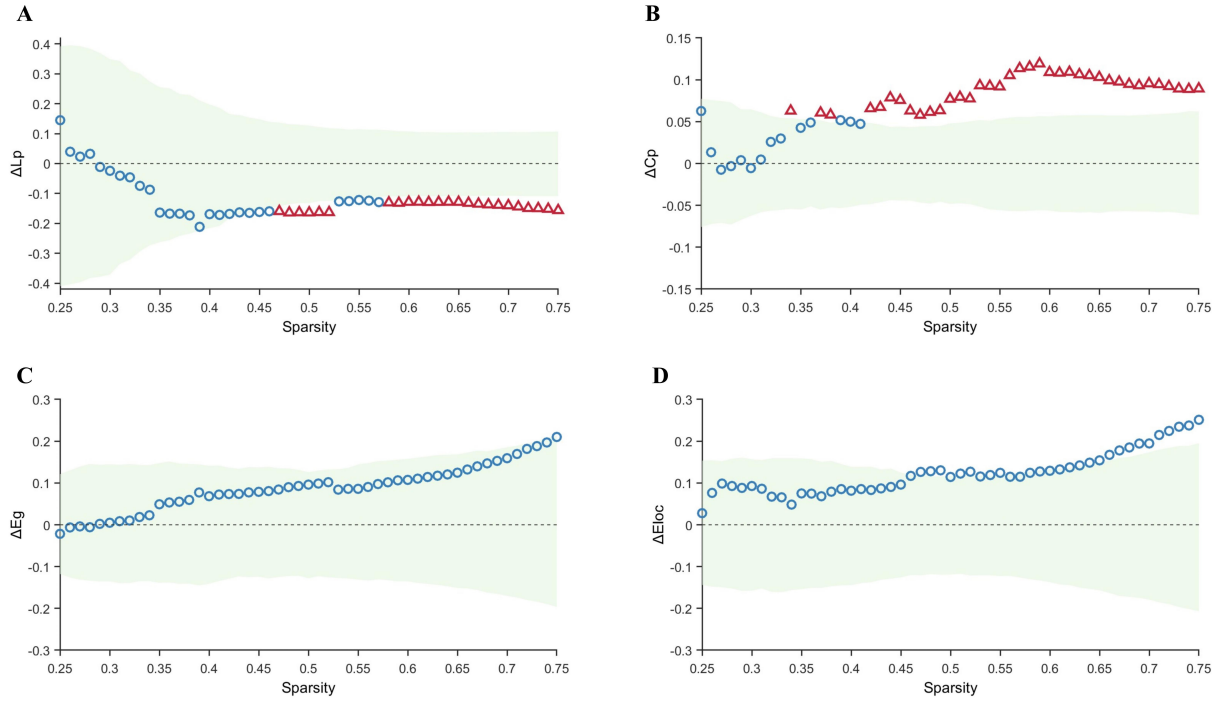

Fig. 2. Comparison of graph-theoretical metrics between the control and TLE-IAS groups. (A–D) Differences and confidence intervals of Lp, Cp, Eg, and Eloc values between the control group and the TLE-IAS group within the sparsity range of 0.25–0.75. The green area represents the 95% CI, red triangles represent significant between-group differences at each sparsity level ($p_{FDR} < 0.05$), while blue circles indicate non-significant between-group differences at each sparsity level. Lp, characteristic path length; Cp, clustering coefficient; Eg, global efficiency; Eloc, local efficiency; CI, confidence intervals.

creased Cp and Eloc values, without any significant difference in Eg (Fig. 3). Sensitivity analysis using bootstrap resampling (1000 iterations) confirmed the robustness of these differences. The 95% confidence intervals (CI) for the area under the difference curve were [0.0061, 0.0350] for Lp, [0.0401, 0.1220] for Cp, and [0.1800, 0.4972] for Eloc, indicating stable overall intergroup differences. Furthermore, after FDR correction across sparsity levels, Lp and Eloc showed significant intergroup differences throughout the entire sparsity range (p_{FDR} ranges: 0.012–0.021 and 0.032–0.037, respectively; with mean ΔLp: –0.3561, mean ΔEloc: 0.2618). The Cp exhibited significant differences at specific sparsity (0.32–0.75) (p_{FDR}: 0.007–0.045; mean ΔCp: 0.1514). In contrast, no significant intergroup differences were found for Eg at any sparsity level (all $p >$ 0.05).

Direct comparison between the TLE-AS and TLE-IAS groups revealed no statistically significant intergroup differences in Lp, Cp, Eg, or Eloc (Fig. 4).

3.4 Hub Node Analysis

Hub nodes, characterized by high centrality, play a key role in information integration and relay within brain networks. In this study, hub nodes were defined at the group level as nodes with Bc values greater than twice the mean Bc and surviving permutation testing.

To compare the hub nodes, a common sparsity threshold of 0.48 was applied, defined as the minimum value ensuring a global efficiency >0.7. The control group contained 13 hubs at this threshold, whereas the number of hubs was reduced to 8 in the TLE-AS and TLE-IAS groups (Fig. 5, Table 2). In the control group, the hub nodes were widely distributed across the default mode network (angular gyrus, left (ANG.L), precuneus, right (PCUN.R), posterior cingulate gyrus, left (PCG.L), etc.), other higher-level association cortices (superior temporal gyrus, left (STG.L), fusiform gyrus, left (FFG.L), cuneus, left (CUN.L)), and additionally spread across the limbic/paralimbic system and subcortical nuclei. In the TLE-IAS group, 6 out of 8 hub nodes were located in the limbic/paralimbic system, followed by subcortical nuclei and limited primary auditory areas (Heschl gyrus, left (HES.L)). Similarly, in the TLE-AS group, 5 out of 8 hub nodes were in the limbic/paralimbic system, including the subcortical nuclei, but the primary auditory cortex (HES.L and Heschl gyrus, right (HES.R)) showed a bilateral distribution.

Compared with the control group, both TLE patient groups exhibited a consistent loss of hub nodes in the default mode network and a widespread reduction of hubs in other higher-order association cortices. Concurrently, the overall hub distribution shifted toward limbic and paralimbic regions, accompanied by the emergence of new hub

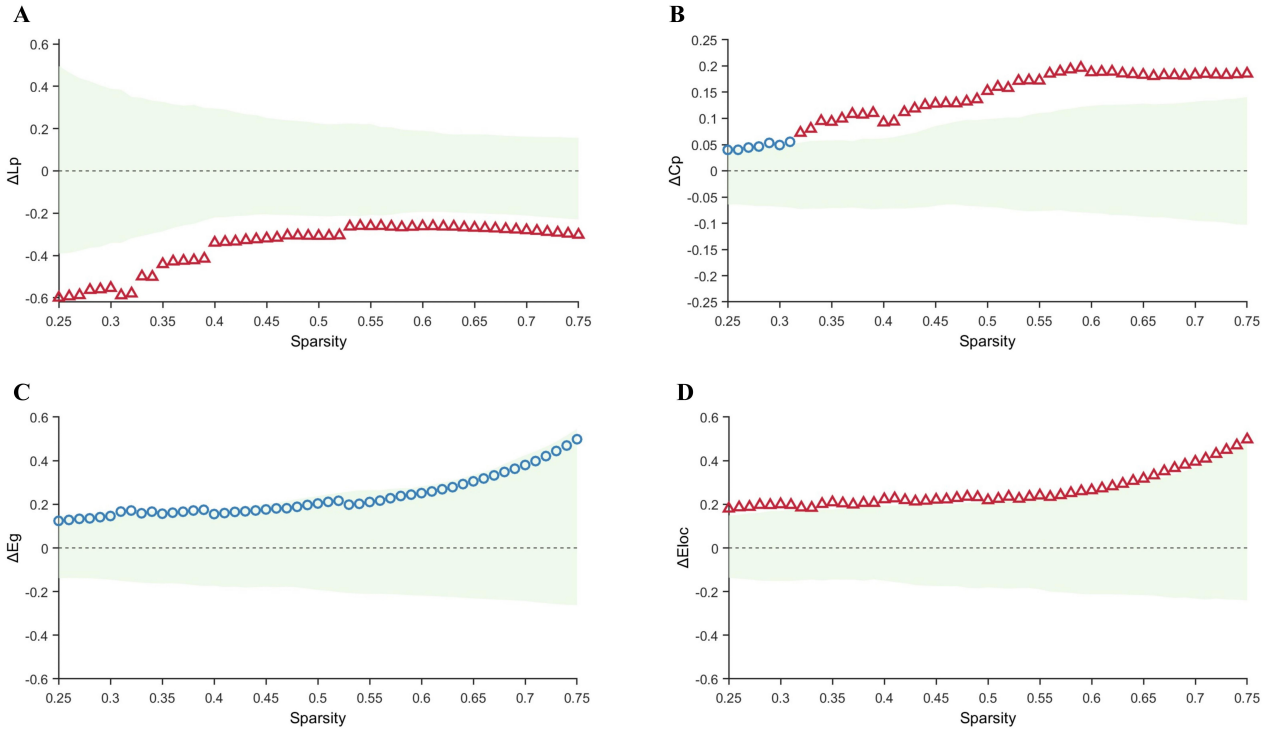

Fig. 3. Comparison of graph-theoretical metrics between the control and TLE-AS groups. (A–D) Differences and confidence intervals of Lp, Cp, Eg, and Eloc values between the control group and the TLE-AS group within the sparsity range of 0.25–0.75. The green area represents the 95% CI, red triangles represent significant between-group differences at each sparsity level ($p_{FDR} < 0.05$), while blue circles indicate non-significant between-group differences at each sparsity level.

nodes in the primary auditory cortex. Additionally, differences in hub composition were observed between both patient groups: the TLE-IAS group exhibited two limbic hubs compared to one in the TLE-AS group, while the TLE-AS group had two primary auditory hubs compared to one in the TLE-IAS group.

4. Discussion

This study used ^{18}F-FDG PET to construct metabolic brain networks. To our knowledge, for the first time, we systematically compared the global topological properties and hub node distributions between TLE-AS and TLE-IAS patients. The main findings can be summarized as follows: both patient groups exhibited reduced network efficiency and a widespread loss of hub nodes in the default mode network and higher-order association cortices. However, key differences were observed in hub reorganization patterns between both patient groups: the TLE-IAS group had a greater number of hubs within the limbic system, whereas the TLE-AS group had more hubs in the primary auditory cortex (with a bilateral distribution).

Recently, awareness during epileptic seizures has attracted growing research interest [31,32]. According to the ILAE, awareness is assessed based primarily on postictal recall, excluding responsiveness, since patients may be aware but unable to respond due to behavioral arrest [2]. However, Contreras *et al.* [33] found that most clinicians assess both ictal responsiveness and postictal recall when classifying focal seizures. Therefore, consistent with previous studies [21,34], we defined impaired awareness seizures as those involving reduced responsiveness to verbal questions, inability to follow commands, or failure to recall ictal experiences.

4.1 Alterations in Metabolic Connectivity and Graph-theoretical Metrics

PET-based analysis of the metabolic brain network offers high robustness and reproducibility [25], partly due to its independence from neurovascular coupling and the whole-brain coverage provided by ^{18}F-FDG PET. This study revealed that compared to controls, both patient groups exhibited widespread disturbances in metabolic connectivity, suggesting impaired large-scale functional coherence in TLE. Graph-theoretic analysis further demonstrated that both patients with TLE-IAS and TLE-AS shared a similar pattern of network impairment, characterized by increased Lp and decreased Cp, reflecting longer communication distances and reduced local integration efficiency. These findings align with previous studies on brain networks in epilepsy [35–37].

Notably, a direct comparison between the TLE-IAS and TLE-AS groups revealed no significant differences in

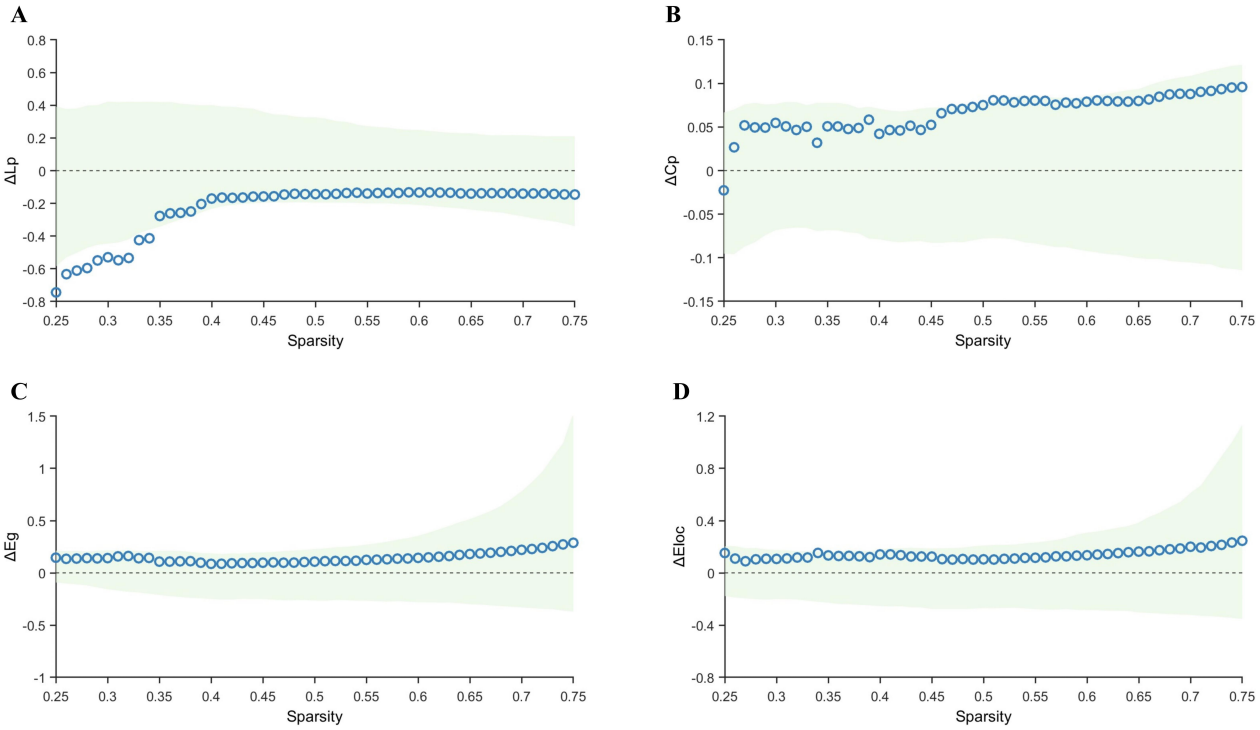

Fig. 4. Comparison of graph-theoretical metrics between the TLE-AS and TLE-IAS groups. (A–D) Differences and confidence intervals of Lp, Cp, Eg, and Eloc values between the TLE-AS and the TLE-IAS group within the sparsity range of 0.25–0.75. The green area represents the 95% CI, red triangles represent significant between-group differences at each sparsity level ($p_{FDR} < 0.05$), while blue circles indicate non-significant between-group differences at each sparsity level.

any of the four graph-theoretical parameters. This suggests that the overall severity of network impairment at the topological level is similar in both patient groups. This pattern differs from the weakening of network connectivity reported in patients with pharmacologically induced unconsciousness. A plausible explanation is that the chronic and widespread network damage caused by TLE may constitute a dominant pathological background, masking the more subtle or state-specific topological changes related to varying degrees of awareness. Additionally, since all imaging data were acquired during the interictal period, dynamic network alterations directly driven by impaired awareness may be less pronounced than those seen in pharmacological models. Therefore, future studies should aim to identify awareness-sensitive topological properties and subnetworks [38], or incorporate multimodal recordings (e.g., ictal EEG) to capture dynamic changes in brain networks.

4.2 Hub Reorganization: Overall Alterations in TLE and Intergroup Differences

Hub nodes, which concentrate numerous shortest paths, are critical for efficient information exchange in the brain. First, compared with the control group, the TLE-IAS and TLE-AS groups exhibited a similar pattern of network reorganization, including the loss of hub nodes in the default mode network and the superior parietal cortex, with hub distribution converging toward the limbic and paralimbic systems. This finding is consistent with previous studies reporting weakened connectivity or functional abnormalities in default mode networks across multiple epilepsy subtypes [39,40]. Furthermore, it corroborates earlier observations that in patients with TLE, the hub nodes predominantly exist in the paralimbic/limbic systems [41], supporting Bonilha *et al.*'s proposed reorganization [42] of limbic regions in TLE. This study also revealed a reduction in hub nodes within the subcortical basal ganglia region across both patient groups (only 1 retained versus 2 in controls), consistent with previous reports showing diminished node strength in this area among epileptics [43]. Regarding the newly identified hub nodes in the primary auditory cortex across both patient groups, we propose that their emergence may compensate for reduced whole-brain integration efficiency and the loss of hub nodes in higher association cortices or may relate to the frequent auditory aura symptoms observed in patients with TLE. Based on the above discussion of the similar pattern in TLE, we propose a preliminary hypothesis that this pattern may facilitate the propagation of epileptic discharges through the limbic/paralimbic system. Further, compensatory alterations in the primary auditory cortex may indicate abnormal discharges in this region during seizures, potentially contributing to auditory auras and other abnormal perceptions. Future studies should fur-

Table 1. General data of the study participants [n (%)].

Characteristics	Control group (n = 193)	TLE-IAS group (n = 193)	TLE-AS group (n = 30)	*p*
Age (years, Mean ± SD)	24.0 (15.0, 33.0)	24.0 (15.0, 33.0)	16.0 (12.0, 35.0)	0.286
Sex				0.919
Male	101 (52.3%)	101 (52.3%)	16 (53.3%)	
Female	92 (47.7%)	92 (47.7%)	14 (46.7%)	
Onset age of seizure (years)	-	14.0 (8.8, 26.0)	13.0 (9.0, 23.0)	0.673
Duration of seizure (years)	-	5.0 (1.0, 10.2)	2.5 (1.0, 8.0)	0.126
MRI				0.835
Positive	-	126 (65.3%)	19 (63.3%)	
Negative	-	67 (34.7%)	11 (36.7%)	

p-values represent comparisons between the TLE-AS and TLE-IAS groups. Sex: $\chi^2(1) = 0.010$, $\varphi = 0.007$; MRI: $\chi^2(1) = 0.043$, $\varphi = 0.014$. TLE, temporal lobe epilepsy; IAS, impaired awareness seizures; AS, aware seizures; MRI, magnetic resonance imaging.

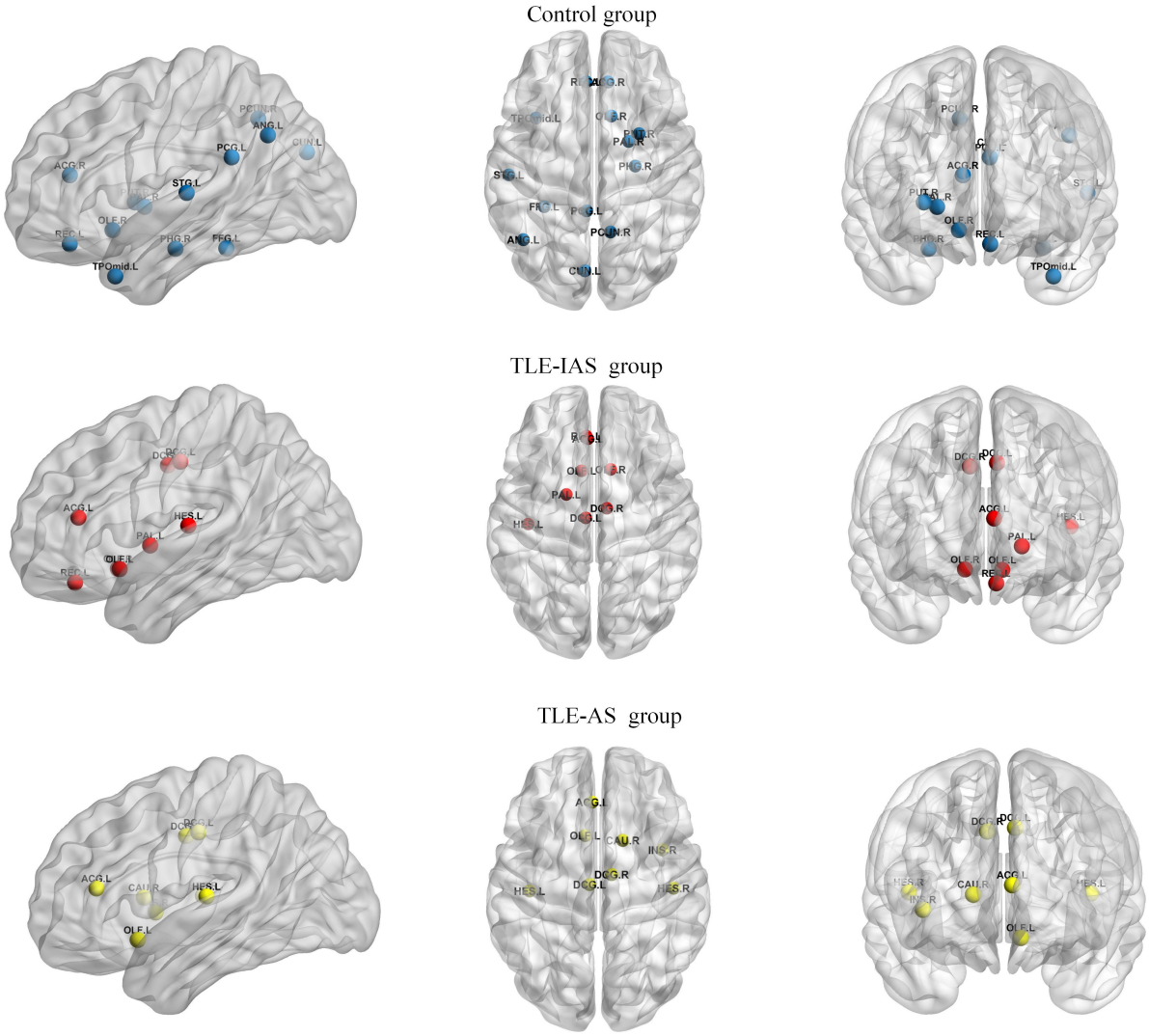

Fig. 5. Hub nodes in the control, TLE-IAS, and TLE-AS groups. Blue, red, and yellow spheres represent hub nodes in the control, TLE-IAS, and TLE-AS groups, respectively.

ther examine the relationship between auditory cortex hub formation and specific clinical symptoms by including a subgroup of patients with auditory aura or by integrating seizure-period EEG data.

Table 2. Distribution of hub nodes in the metabolic networks of each group.

Brain Region	Abbreviation	Functional classification	Control Group	TLE-IAS Group	TLE-AS Group
Olfactory cortex, left	OLF.L	Limbic	-	✓	✓
Olfactory cortex, right	OLF.R	Limbic	✓	✓	-
Gyrus rectus, left	REC.L	Paralimbic	✓	✓	-
Anterior cingulate and paracingulate gyri, left	ACG.L	Paralimbic	-	✓	✓
Anterior cingulate and paracingulate gyri, right	ACG.R	Paralimbic	✓	-	-
Median cingulate and paracingulate gyri, left	DCG.L	Paralimbic	-	✓	✓
Median cingulate and paracingulate gyri, right	DCG.R	Paralimbic	-	✓	✓
Posterior cingulate gyrus, left	PCG.L	Paralimbic	✓	-	-
Insula, right	INS.R	Paralimbic	-	-	✓
Parahippocampal gyrus, right	PHG.R	Paralimbic	✓	-	-
Temporal pole: middle temporal gyrus, left	TPOmid.L	Paralimbic	✓	-	-
Caudate nucleus, right	CAU.R	Subcortical	-	-	✓
Putamen, right	PUT.R	Subcortical	✓	-	-
Pallidum, left	PAL.L	Subcortical	-	✓	-
Pallidum, right	PAL.R	Subcortical	✓	-	-
Cuneus, left	CUN.L	Association	✓	-	-
Fusiform gyrus, left	FFG.L	Association	✓	-	-
Angular gyrus, left	ANG.L	Association	✓	-	-
Precuneus, right	PCUN.R	Association	✓	-	-
Superior temporal gyrus, left	STG.L	Association	✓	-	-
Heschl gyrus, left	HES.L	Primary/Auditory	-	✓	✓
Heschl gyrus, right	HES.R	Primary/Auditory	-	-	✓

Check marks (✓) indicate brain regions identified as hub nodes.

The difference in hub distribution between the TLE-IAS and TLE-AS groups provides preliminary insights into the neural substrates underlying their distinct awareness states. Compared to the TLE-IAS group, which exhibited only one additional hub in the primary auditory cortex, the TLE-AS group showed two new hubs in the bilateral primary auditory cortex (HES.L and HES.R), which may provide the neural network foundation for maintaining basic awareness and sensory processing during epileptic seizures. Moreover, compared to the control and TLE-AS groups, the TLE-IAS group exhibited a higher number of hub nodes in the limbic system. This might be due to an accumulation of pathological states. However, whether this difference is directly related to impaired awareness or attributable to epileptic burden remains unclear. Future studies should validate this finding by controlling for key variables, such as seizure frequency and medication use, or expanding the sample size of patients with TLE-AS. Recently, two major hypotheses have been proposed to explain impaired awareness during seizures: the "network inhibition hypothesis" [18] and the "global workspace theory" [17], which collectively highlight the importance of the frontal cortex in the awareness system. However, in contrast to these theories, we observed that REC.L, a hub node in the prefrontal cortex, was specifically lost in the TLE-AS group, whereas it was present in both the control and TLE-IAS groups. Given the limitations of the current cross-sectional study design, the specific mechanisms underlying this phenomenon are difficult to fully explain. To avoid overinterpretation, we present this finding here as a critical observation, warranting targeted experimental designs to underscore its exact significance.

4.3 Limitations

This study has several limitations. First, the sample size of the TLE-AS group is relatively small, mainly due to the low prevalence of TLE-AS in clinical settings and limited PET/CT utilization in this subgroup. Although bootstrap resampling was applied to improve robustness, future studies should aim to expand this cohort to strengthen the conclusions. Second, the network analysis was conducted at the group level, potentially overlooking individual variability. In the future, individualized network approaches, such as those based on Kullback–Leibler divergence, can be adopted to capture subject-specific topological profiles. Third, given the radiation exposure associated with PET/CT, control subjects were recruited from patients without neuropsychiatric conditions rather than healthy volunteers. Even with careful age- and sex-matching, unmeasured confounders may persist. Fourth, although the broad age range (6–65 years) was similar to that of some related studies and showed no statistically significant intergroup differences, developmental differences in the brain metabolic network between children and adults might intro-

duce confounding effects. Finally, owing to the retrospective nature of the study, several clinically relevant variables (e.g., seizure side, medication regimen, seizure frequency, and surgical pathological or stereo-electroencephalography findings) were not systematically controlled. These factors might preclude precise localization of the seizure onset zone for causal inference and may introduce variability in metabolic network patterns, which should be accounted for in future prospective designs.

5. Conclusions

This study reveals distinct patterns of metabolic brain network reorganization in TLE-IAS and TLE-AS. Graph-theoretic analysis revealed that both patient groups exhibited weaker global metabolic connectivity and lower network efficiency than the controls. Regarding hub node distribution, both groups demonstrated loss of hub nodes in the default mode network and the superior parietal cortex, with distribution shifting toward the limbic/paralimbic system. Compared to the TLE-AS group, the TLE-IAS group showed no significant differences in graph theory parameters. However, the hub nodes in the TLE-IAS group were more prevalent in the limbic system, whereas they were primarily found in the primary auditory cortex in the TLE-AS group. These findings provide novel metabolic imaging-based evidence for understanding the neural basis of impaired awareness in TLE and establish a theoretical framework for future targeted interventions. Future studies should validate these network characteristics through balanced patient cohorts and prospective designs, translating them into practical tools for clinical precision diagnosis and treatment stratification.

Availability of Data and Materials

The datasets used and analyzed in the present study are available upon request from the corresponding author.

Author Contributions

JX and JL designed the research study. JX and FY performed the research. FY provided help and advice on visualization. HZ analyzed the data. JX and FY wrote the manuscript. JL provided project administration and funding acquisition. All authors contributed to editorial changes in the manuscript. All authors read and approved the final manuscript. All authors have participated sufficiently in the work and agreed to be accountable for all aspects of the work.

Ethics Approval and Consent to Participate

The study was conducted in accordance with the Declaration of Helsinki. The research protocol was approved by the Ethics Committee of Medical Ethics Experts of the Second Hospital of Lanzhou University (Ethic Approval Number: 2025A-141), and all of the participants provided signed informed consent.

Acknowledgment

The authors thank all the participants for their assistance and cooperation with our study.

Funding

This research was funded by the Joint Funds of the Science and Technology Program of Gansu Province (Grant No. 24JRRA922) and the Science and Technology Program of Gansu Province (Grant No. 23ZDFA003).

Conflict of Interest

The authors declare no conflict of interest.

Declaration of AI and AI-Assisted Technologies in the Writing Process

During the preparation of this work, the authors utilized DeepSeek for spelling and grammar checks and employed ChatGPT-5.0 for English language polishing. After using these tools, the authors reviewed and edited the content as necessary and take full responsibility for the publication's content.

Supplementary Material

Supplementary material associated with this article can be found, in the online version, at https://doi.org/10.31083/JIN47320.

References

[1] Krishnamurthy KB. Epilepsy. Annals of Internal Medicine. 2025; 178: ITC49–ITC64. https://doi.org/10.7326/ANNALS-25-00494.

[2] Fisher RS, Cross JH, D'Souza C, French JA, Haut SR, Higurashi N, *et al*. Instruction manual for the ILAE 2017 operational classification of seizure types. Epilepsia. 2017; 58: 531–542. https://doi.org/10.1111/epi.13671.

[3] Blumenfeld H, Meador KJ. Consciousness as a useful concept in epilepsy classification. Epilepsia. 2014; 55: 1145–1150. https://doi.org/10.1111/epi.12588.

[4] Wang Y, Chen Y, Cui Y, Zhao T, Wang B, Zheng Y, *et al*. Alterations in electroencephalographic functional connectivity in individuals with major depressive disorder: a resting-state electroencephalogram study. Frontiers in Neuroscience. 2024; 18: 1412591. https://doi.org/10.3389/fnins.2024.1412591.

[5] Horwitz B. The elusive concept of brain connectivity. NeuroImage. 2003; 19: 466–470. https://doi.org/10.1016/s1053-8119(03)00112-5.

[6] Lee DS, Kang H, Kim H, Park H, Oh JS, Lee JS, *et al*. Metabolic connectivity by interregional correlation analysis using statistical parametric mapping (SPM) and FDG brain PET; methodological development and patterns of metabolic connectivity in adults. European Journal of Nuclear Medicine and Molecular Imaging. 2008; 35: 1681–1691. https://doi.org/10.1007/s00259-008-0808-z.

[7] Ponisio MR, Zempel JM, Day BK, Eisenman LN, Miller-Thomas MM, Smyth MD, *et al*. The Role of SPECT and PET in Epilepsy. AJR. American Journal of Roentgenology. 2021; 216: 759–768. https://doi.org/10.2214/AJR.20.23336.

[8] Carli G, Tondo G, Boccalini C, Perani D. Brain Molecular

Connectivity in Neurodegenerative Conditions. Brain Sciences. 2021; 11: 433. https://doi.org/10.3390/brainsci11040433.

[9] Zhang W, Duan Y, Qi L, Li Z, Ren J, Nangale N, *et al*. Distinguishing Patients with MRI-Negative Temporal Lobe Epilepsy from Normal Controls Based on Individual Morphological Brain Network. Brain Topography. 2023; 36: 554–565. https://doi.org/10.1007/s10548-023-00962-z.

[10] Guo Y, Lin Z, Fan Z, Tian X. Epileptic brain network mechanisms and neuroimaging techniques for the brain network. Neural Regeneration Research. 2024; 19: 2637–2648. https://doi.org/10.4103/1673-5374.391307.

[11] Mittal P, Gautam RK, Sharma H, Goyal R, Garima, Kapoor R, *et al*. Neural Networks of Knowledge: Ontologies Pioneering Precision Medicine in Neurodegenerative Diseases. Current Neuropharmacology. 2025; 23: 1878–1893. https://doi.org/10.2174/011570159X353727250314065140.

[12] de Palma L, De Benedictis A, Specchio N, Marras CE. Epileptogenic Network Formation. Neurosurgery Clinics of North America. 2020; 31: 335–344. https://doi.org/10.1016/j.nec.2020.03.012.

[13] Moosavi SA, Jirsa VK, Truccolo W. Critical dynamics in the spread of focal epileptic seizures: Network connectivity, neural excitability and phase transitions. PloS One. 2022; 17: e0272902. https://doi.org/10.1371/journal.pone.0272902.

[14] Piper RJ, Richardson RM, Worrell G, Carmichael DW, Baldeweg T, Litt B, *et al*. Towards network-guided neuromodulation for epilepsy. Brain: a Journal of Neurology. 2022; 145: 3347–3362. https://doi.org/10.1093/brain/awac234.

[15] Farahani FV, Karwowski W, Lighthall NR. Application of Graph Theory for Identifying Connectivity Patterns in Human Brain Networks: A Systematic Review. Frontiers in Neuroscience. 2019; 13: 585. https://doi.org/10.3389/fnins.2019.00585.

[16] Nigro S, Filardi M, Tafuri B, De Blasi R, Cedola A, Gigli G, *et al*. The Role of Graph Theory in Evaluating Brain Network Alterations in Frontotemporal Dementia. Frontiers in Neurology. 2022; 13: 910054. https://doi.org/10.3389/fneur.2022.910054.

[17] Bartolomei F, Naccache L. The global workspace (GW) theory of consciousness and epilepsy. Behavioural Neurology. 2011; 24: 67–74. https://doi.org/10.3233/BEN-2011-0313.

[18] Yu L, Blumenfeld H. Theories of impaired consciousness in epilepsy. Annals of the New York Academy of Sciences. 2009; 1157: 48–60. https://doi.org/10.1111/j.1749-6632.2009.04472.x.

[19] Xie F, Xing W, Wang X, Liao W, Shi W. Altered states of consciousness in epilepsy: a DTI study of the brain. The International Journal of Neuroscience. 2017; 127: 667–672. https://doi.org/10.1080/00207454.2016.1229668.

[20] Campora N, Princich JP, Nasimbera A, Cordisco S, Villanueva M, Oddo S, *et al*. Stereo-EEG features of temporal and frontal lobe seizures with loss of consciousness. Neuroscience of Consciousness. 2024; 2024: niae003. https://doi.org/10.1093/nc/niae003.

[21] Hou J, Zhu H, Xiao L, Zhao CW, Liao G, Tang Y, *et al*. Alterations in Cortical-Subcortical Metabolism in Temporal Lobe Epilepsy With Impaired Awareness Seizures. Frontiers in Aging Neuroscience. 2022; 14: 849774. https://doi.org/10.3389/fnagi.2022.849774.

[22] Seth AK. Consciousness: The last 50 years (and the next). Brain and Neuroscience Advances. 2018; 2: 2398212818816019. https://doi.org/10.1177/2398212818816019.

[23] Kong Y, Chen Z, Zhang J, Wang Y, Chu M, Nan H, *et al*. Reconfigured metabolism brain network in asymptomatic Creutzfeldt-Jakob disease. Neurobiology of Disease. 2025; 206: 106805. https://doi.org/10.1016/j.nbd.2025.106805.

[24] Ren S, Huang Q, Bao W, Jiang D, Xiao J, Li J, *et al*. Metabolic Brain Network and Surgical Outcome in Temporal Lobe Epilepsy: A Graph Theoretical Study Based on ^{18}F-fluorodeoxyglucose PET. Neuroscience. 2021; 478: 39–48. https://doi.org/10.1016/j.neuroscience.2021.10.012.

[25] Wang XW. Follow-up Studies of 18F-FDG PET and Metabolic Network Connectivity in Pediatric Epilepsy [Dissertation]. Zhejiang University: Zhejiang. 2021. https://doi.org/10.27461/d.cnki.gzjdx.2021.003523.

[26] Sun Y, Shi Q, Ye M, Miao A. Topological properties and connectivity patterns in brain networks of patients with refractory epilepsy combined with intracranial electrical stimulation. Frontiers in Neuroscience. 2023; 17: 1282232. https://doi.org/10.3389/fnins.2023.1282232.

[27] Wang J, Wang X, Xia M, Liao X, Evans A, He Y. GRETNA: a graph theoretical network analysis toolbox for imaging connectomics. Frontiers in Human Neuroscience. 2015; 9: 386. https://doi.org/10.3389/fnhum.2015.00386.

[28] Sone D, Matsuda H, Ota M, Maikusa N, Kimura Y, Sumida K, *et al*. Graph Theoretical Analysis of Structural Neuroimaging in Temporal Lobe Epilepsy with and without Psychosis. PloS One. 2016; 11: e0158728. https://doi.org/10.1371/journal.pone.0158728.

[29] Yao Z, Zhang Y, Lin L, Zhou Y, Xu C, Jiang T, *et al*. Abnormal cortical networks in mild cognitive impairment and Alzheimer's disease. PLoS Computational Biology. 2010; 6: e1001006. https://doi.org/10.1371/journal.pcbi.1001006.

[30] Xia M, Wang J, He Y. BrainNet Viewer: a network visualization tool for human brain connectomics. PloS One. 2013; 8: e68910. https://doi.org/10.1371/journal.pone.0068910.

[31] Varotto G, Burini A, Didato G, Deleo F, Pastori C, Dominese A, *et al*. Impaired awareness in mesial temporal lobe epilepsy: Network analysis of foramen ovale and scalp EEG. Clinical Neurophysiology: Official Journal of the International Federation of Clinical Neurophysiology. 2021; 132: 3084–3094. https://doi.org/10.1016/j.clinph.2021.09.011.

[32] Sieu LA, Singla S, Liu J, Zheng X, Sharafeldin A, Chandrasekaran G, *et al*. Slow and fast cortical cholinergic arousal is reduced in a mouse model of focal seizures with impaired consciousness. Cell Reports. 2024; 43: 115012. https://doi.org/10.1016/j.celrep.2024.115012.

[33] Contreras Ramirez V, Vaddiparti A, Blumenfeld H. Testing awareness in focal seizures: Clinical practice and interpretation of current guidelines. Annals of Clinical and Translational Neurology. 2022; 9: 762–765. https://doi.org/10.1002/acn3.51552.

[34] Englot DJ, Yang L, Hamid H, Danielson N, Bai X, Marfeo A, *et al*. Impaired consciousness in temporal lobe seizures: role of cortical slow activity. Brain: a Journal of Neurology. 2010; 133: 3764–3777. https://doi.org/10.1093/brain/awq316.

[35] Slinger G, Otte WM, Braun KPJ, van Diessen E. An updated systematic review and meta-analysis of brain network organization in focal epilepsy: Looking back and forth. Neuroscience and Biobehavioral Reviews. 2022; 132: 211–223. https://doi.org/10.1016/j.neubiorev.2021.11.028.

[36] Jelsma SB, Zijlmans M, Heijink IB, Hoefnagels FWA, Raemaekers M, Otte WM, *et al*. Structural and effective brain connectivity in focal epilepsy. Neuroimage. Reports. 2025; 5: 100274. https://doi.org/10.1016/j.ynirp.2025.100274.

[37] Pegg EJ, McKavanagh A, Bracewell RM, Chen Y, Das K, Denby C, *et al*. Functional network topology in drug resistant and well-controlled idiopathic generalized epilepsy: a resting state functional MRI study. Brain Communications. 2021; 3: fcab196. https://doi.org/10.1093/braincomms/fcab196.

[38] Wang X, Lin D, Zhao C, Li H, Fu L, Huang Z, *et al*. Abnormal metabolic connectivity in default mode network of right temporal lobe epilepsy. Frontiers in Neuroscience. 2023; 17: 1011283. https://doi.org/10.3389/fnins.2023.1011283.

[39] Zanão TA, Lopes TM, de Campos BM, Yasuda CL, Cendes F. Patterns of default mode network in temporal lobe epilepsy with and without hippocampal sclerosis. Epilepsy & Behavior: E&B. 2021; 121: 106523. https://doi.org/10.1016/j.yebeh.2019.106523.

[40] Parsons N, Bowden SC, Vogrin S, D'Souza WJ. Default mode network dysfunction in idiopathic generalised epilepsy. Epilepsy Research. 2020; 159: 106254. https://doi.org/10.1016/j.eplepsyres.2019.106254.

[41] Yasuda CL, Chen Z, Beltramini GC, Coan AC, Morita ME, Kubota B, *et al*. Aberrant topological patterns of brain structural network in temporal lobe epilepsy. Epilepsia. 2015; 56: 1992–2002. https://doi.org/10.1111/epi.13225.

[42] Bonilha L, Nesland T, Martz GU, Joseph JE, Spampinato MV, Edwards JC, *et al*. Medial temporal lobe epilepsy is associated with neuronal fibre loss and paradoxical increase in structural connectivity of limbic structures. Journal of Neurology, Neurosurgery, and Psychiatry. 2012; 83: 903–909. https://doi.org/10.1136/jnnp-2012-302476.

[43] Výtvarová E, Mareček R, Fousek J, Strýček O, Rektor I. Large-scale cortico-subcortical functional networks in focal epilepsies: The role of the basal ganglia. NeuroImage. Clinical. 2017; 14: 28–36. https://doi.org/10.1016/j.nicl.2016.12.014.